

AN INTELLIGENT HAIR AND SCALP ANALYSIS SYSTEM USING CAMERA SENSORS AND NORWOOD-HAMILTON MODEL

SHIH-HSIUNG LEE^{1,2} AND CHU-SING YANG^{1,2}

¹Institute of Computer and Communication Engineering

²Department of Electrical Engineering

National Cheng Kung University

No. 1, University Road, Tainan City 701, Taiwan

beargoer@gmail.com; csyang@ee.ncku.edu.tw

Received August 2017; revised December 2017

ABSTRACT. *With the rapid development of information technology and sensors, new types of medical services have been introduced to users. Baldness or hair loss has caused significant problems for people on social occasions and even affected their health. Therefore, hair and scalp care are taken more seriously by people. Hair care or scalp detection can be realized in a professional hair care shop or medical and cosmetic clinic, but it is very expensive. Recently, owing to the enhancement in computation ability of intelligent devices and decrease in prices, it is feasible to have an inexpensive hair and scalp analysis system. This paper proposes the concept of using webcam and microscope camera sensors to extract characteristic images to evaluate the hair and scalp status of the user. Through the Norwood-Hamilton scale model and detection of scalp surface status, actual information is provided to the users to understand their own physical status. Additionally, this system uses an NVidia Jetson TK1 platform as the master device to increase computing efficiency, which is a new solution. In this work, experiments are conducted to verify the validity and feasibility of the system.*

Keywords: Hair diagnosis, Scalp diagnosis, Image processing, Lighting condition estimation, Hair and scalp analysis system

1. Introduction. Increasing improvements in the processing technology of biomedical images have led to the development of new types of medical services. Image analysis and high-accuracy auxiliary systems can be relied on to effectively aid doctors in making a better diagnosis and taking decisions for the patients. The human hair image is a very complex visual pattern [1] where thousands of hairs form numerous hairstyles. Different factors including age, gender, disease, genetics, pressure, abuse of hair care products, malnutrition, and living in different climate regions may cause hair loss. In recent years, the problem of hair loss is increasingly occurring at a younger age. A progressively receding hairline and thinning of the hair increase the visual age, resulting in a loss of confidence. Therefore, the emphasis on hair and scalp care is currently growing, and people often search for solutions in hair care shops or at medical and cosmetic clinics. However, the treatments are extremely expensive and unaffordable, and consequently, the appropriate time for hair loss treatment gets delayed causing baldness or affecting health. The Norwood-Hamilton scale model in [2,3] is a type of method to measure the male baldness degree; it is also the generally accepted standard to describe hair loss. According to the definition of Phase 7 baldness, for Phase 5 baldness or above, the best practical solution is transplanting hair or wearing wigs. Therefore, it is suggested to use drugs or other treatment methods when the baldness is within Phase 2, which is considered as the golden phase for hair treatment. The scalp is one of the skin tissues

of the human body, and hair loss is caused by external factors or the health conditions of the affected person. Common scalp problems include seborrheic dermatitis, folliculitis, psoriasis, scalp allergy, oily scalp, and dry scalp. Therefore, there is a steady growth in the products and research that can provide consumers with inexpensive equipment for rapid scalp diagnosis as reported in [4-7]. Hair is an obstacle in the clinical diagnosis of scalp. Hence, a lot of research works focus on hair segmentation and removal as referred in [17,18]. It would be useful for the effective feature extraction and classification. To further analyze a scalp image, many research works considered the scalp status, such as the health status, density, diameter, oiliness, and hair quantity of each hair follicle. Because the hair density and diameter of a subject usually reflects the health status of scalp, how to count the hair is the most important for a diagnosis system. Hoffmann [20] proposed a type of automatic system for counting the hair. Shih [4] and Kim et al. [6] also proposed the method for counting and measuring hair and scalp. However, it is quite difficult to count hair accurately. In our work, webcam and microscope camera sensors are used to extract a characteristic image. The baldness status of human hair is determined according to the Norwood-Hamilton scale model that is used as a reference for users to utilize the golden phase for treatment. Compared with the hair counting technology, this method is relatively simple and easy, and it mainly considers the holistic hair status. Although in comparison with professional services, their results are dissatisfactory, they are becoming increasingly popular because of their convenience and cost benefits. Moreover, family pets have gradually become common in modern society, and hair loss in pets is also a major problem of concern for numerous pet owners. The image processing technique applied to the human scalp, can also be used suitably by veterinarians to determine a solution for the hair loss in pets.

The main contribution of this study lies in proposing a system for detecting the baldness degree and scalp condition. Webcam and microscope camera sensors were used to extract characteristic images, and an image processing technique was applied for pre-processing and feature comparison to evaluating the hair and scalp status of the subject under study. In the scalp data collected, the scalp was photographed under unknown lighting conditions; differences in the lighting conditions would affect the algorithm, and hence, accurate results could not be obtained directly. Therefore, the support vector machine (SVM) was employed to predict the lighting conditions based on the differences in the colors of the images. It was trained so that the parameter could be adjusted in accordance with different environments. Thus, a certain degree of accuracy could be achieved despite different lighting conditions. In addition, we implemented an easy hair and scalp diagnosis system on an NVidia Jetson TK1 platform and provided a user-friendly operation interface environment.

The remaining paper is organized as follows. Section 2 discusses the background and related works. Section 3 provides the details of the proposed system for detecting the hair and scalp status. The experimental results and analysis are presented in Section 4. Finally, the conclusions of this study are summarized in Section 5.

2. Related Works.

2.1. Hairstyle modeling and synthesis. In the past, most research topics about hair image processing focused on hairstyle modeling and synthesis. Chen and Zhu [1] proposed a generative sketch model for human hair analysis and synthesis. The generative model of hairstyle was divided into three levels (bottom level, middle level, and top level), and one sketch was divided into 11 types of directed primitives. Different hairstyle images were used in one large dataset to test the algorithm, and a simple software interface

was provided, so that inferences or manual inputs (edits) were made based on the real hair image, and the generative model of the real hair image was synthesized. Yeh et al. [8] proposed a concept wherein the novel 2.5D modeling method was adopted to perform the modeling for the hair in the supplied cartoon images and generate various visual effects. For example, the simplified fluid simulation model was used to generate the visual animation effects of blowing 2.5D hair by wind. Yu and Li [9] suggest utilizing a visual emotional synthesis system to synthesize facial expressions by an anatomical and a parameterized model. The mass-spring and cantilever beam models were used to describe emotions in the cartoons. The synthesis results of the facial expressions and hairstyles were combined to obtain the complete visual emotional synthesis results to improve the emotional expressiveness of animation figures. Wang et al. [10] formulated an automatic hair synthesis method that was based on a cluster-oriented theory for hair geometry synthesis, including the conservation and combination of characteristics and detailed transfer of different hairstyles. The hairstyle modeling method may be one of the ways to measuring the shape of baldness. However, the hairstyle of baldness is difficult to model for detecting the level of baldness. Therefore, in this work, the Norwood-Hamilton scale model is used as a reference for users to utilize the golden phase for treatment.

2.2. Hair segmentation and style recognition. In the diagnosis system, the image which includes the hair or non-hair features should be preprocessed to remove the non-hair region. In recent years, researches have been increasingly paying attention to hair segmentation and style recognition. Ahn and Kim [11] proposed a method where semi-supervised spectral clustering multi-segmentation was used to identify the facial and hair regions. Svanera et al. [12] suggested a novel multiclass image database for use in the field of detection of hair, which is known as Figaro. Without using any classifier, the histogram of gradients (HOG) and linear ternary pattern (LTP) information of an image were captured as texture features. Through the random forest method, the image patches were classified into hair and non-hair. Then, the classified patches were improved by the multiple segmentation method based on the image to acquire the results at the pixel level. The above method had significant effects on the experimental results. Proença and Neves [13] used hierarchical Markov random fields (MRFs) to propose soft biometric globally coherent solutions for hair segmentation and style recognition. Other studies on hair segmentation can be found in [14,15]. The preprocessing of hair segmentation is useful for increasing the accuracy rate of baldness detection. However, our target goal is to design a simple and fast diagnosis system. Therefore, we constrain the form of input images to reduce computation effort.

2.3. Scalp skin lesion diagnosis. In a scalp medical image, a skin lesion is mainly analyzed similar to melanoma detection for proposing effective hair segmentation methods and to increase the diagnosis efficiency. Joseph and Panicker [16] suggested a non-invasive automatic skin lesion analysis system in which an image processing technique was used for hair detection and removal for the effective classification and feature extraction of a skin wound. Simultaneously, a fast marching in-painting algorithm was also used for the action of hair removal to improve the accuracy rate of judgment. Hair is an obstacle in the clinical diagnosis of scalp; consequently, numerous research studies reported in the literature mainly discuss hair segmentation and removal, e.g., in [17,18]. Lionnie and Alaydrus [19] proposed an androgenic hair pattern recognition system in which the Haar wavelet transformation was applied to analyzing 400 images of lower right legs. Thus, it can be inferred that the human body hair is of value in scalp analysis. In our work, we aim to design a simple and fast diagnosis system. Therefore, we use the microscope to

constrain the form of input images for reducing the computation effort. However, the hair segmentation for scalp analysis is valued in the scalp medical image diagnosis system.

2.4. Hair counting. To further analyze a scalp image, various researches have in particular considered the scalp status, such as the health status, density, diameter, oiliness, and hair quantity of each hair follicle. Currently, the diagnosis for human hair and scalp mainly relies on the skills and knowledge of a professional scalp evaluator. The hair density and diameter of a subject usually reflects the health status of his scalp. An evaluator manually performs hair counting, but its result is usually unreliable. Furthermore, manual counting cannot determine the hair diameter and length. Hoffmann [20] proposed a type of automatic system for counting the hair on a human body. Shih [4] formulated an automatic standard diagnosis system in which images were obtained via a digital microscope, whereas the hair on the scalp was segmented and counted to determine the hair density, diameter, length, and oiliness level. In addition, a hair-bundling algorithm and relaxation labeling (RL) method have also been proposed. Under various white balances, the bright spots because of oil or moisture on the scalp are captured, and the problem of wavy or curly hair causing overlapping hairs to be considered as single hair, can be avoided. Thus, this algorithm will be more accurate than the Hough line detection algorithm in [21]. Kim et al. [6] proposed a new scheme wherein a microscope image was used to capture multiple features to evaluate the hair and scalp status. These features included hair thickness, hair density, and scalp blotch. Simultaneously, an inexpensive intelligent device prototype was designed to improve the feasibility of self-diagnosis of hair status.

At present, research on hair and scalp status mainly focuses on the separation of hair and scalp, followed by the hair and scalp status analyses. However, it is quite difficult to count hair accurately. In this work, webcam and microscope camera sensors are used to extract a characteristic image. The baldness status of human hair is determined according to the Norwood-Hamilton scale model that is used as a reference for users to utilize the golden phase for treatment. Compared with the hair counting technology, this method is relatively simple and easy, and it mainly considers the holistic hair status. The effect of different lighting environments is analyzed to adjust parameters and detect scalp status. In addition, an easy hair and scalp diagnosis system is implemented on an NVidia Jetson TK1 platform and a user-friendly operation interface environment is provided.

3. Proposed Methods. Figure 1 shows the flowchart of the proposed system, including its two stages. In the pre-processing stage of baldness detection, the clothes or background environment included in the input images will generate noise. To reduce the disturbances, the boundary of the image is cropped through the user interface of the system. Then the Otsu threshold value [24] is used to obtain the binary image, and K-means clustering [25] is performed twice for this binary image. For the detection of the scalp status, the scalp image is converted from the color space to the CIE (International Commission on Illumination) xyY color space, and simultaneously a difference image is generated and a feature vector is output. Next, the lighting condition of this picture is predicted based on the lighting condition classifier already trained well by us. In the detection stage, the baldness status is contrasted according to the Norwood-Hamilton scale model, and the three most possible situations are output. A voting mechanism is adopted against the three situations to obtain the results. In the detection of the scalp status, the parameter is set and adjusted according to the lighting conditions. Then, the previously generated color histogram patterns are recalculated through the histogram back projection and processed through the threshold method; lastly, the recognition results are output.

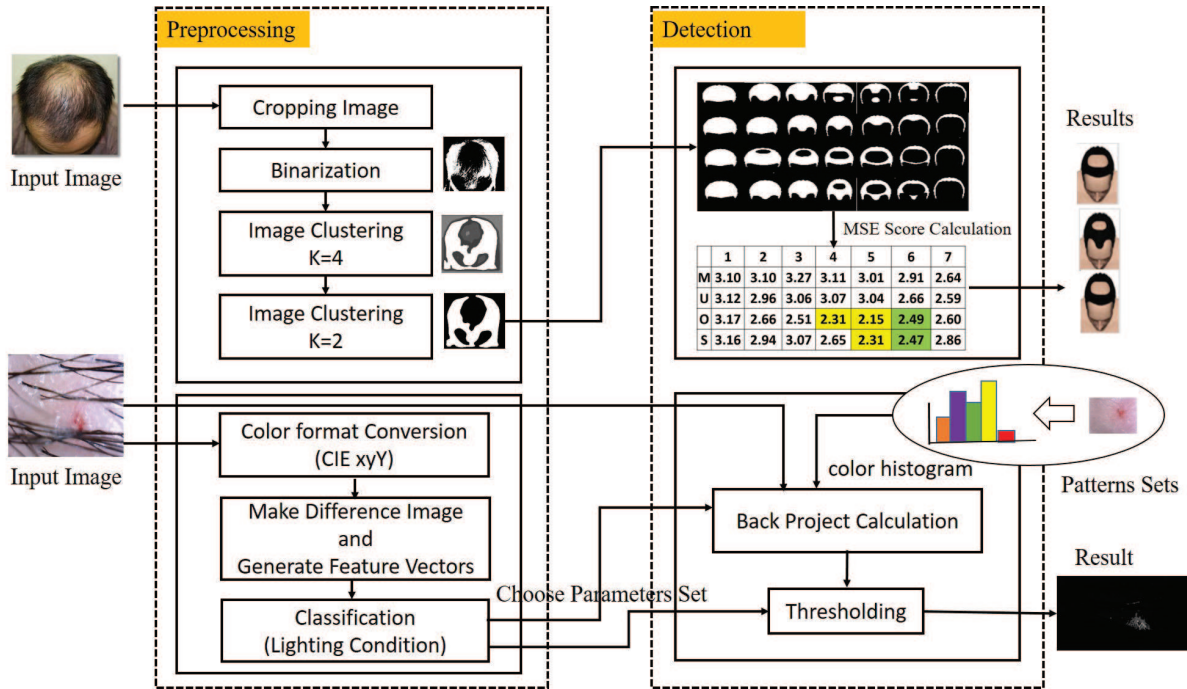


FIGURE 1. Overview of the proposed designed system

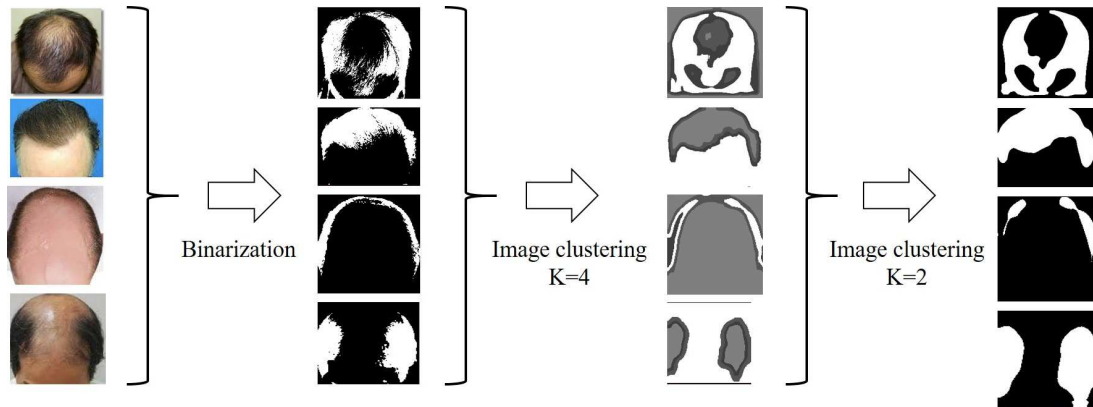


FIGURE 2. Preprocessing flow of clustering of a hair image

3.1. Preprocessing. The clothes of the users and background environment in the images extracted by the webcam will affect the accuracy of the judgment. Therefore, in Step 1, the boundary of the target image is cropped by a user-friendly interface operation provided by the system, and then the Otsu threshold value is used to obtain the binary image. K-means clustering is conducted twice for this binary image with K values of four and two, as shown in Figure 2. We use the K value of four to separate the background environment and hair. Owing to the influence of light condition, the K value of four has the good performance to classify this situation. Again, we do the K-means clustering by setting the K value of two. We would like to get the non-hair and hair result. We expected the outcome of the second step could remove noise more clearly to increase the diagnosis efficiency. In some situations, it is unnecessary to perform the K-means clustering twice; it is only required to divide the binary images into two groups. The image noise that is not on the scalp can be removed more clearly if more than one K-means clustering is

performed. The pre-processing of scalp detection will be discussed in detail in subsection “Parameter adjustment based on different lighting conditions”.

3.2. Detection of baldness status. According to the Norwood-Hamilton scale model shown in Figure 3, the baldness status is divided into seven and four phases, including M type, U type, O type, and syndrome type. According to the Norwood-Hamilton scale model, the 7-phase baldness model images become the contrastive sample images after binarization, as shown in Figure 4. After the hair images of the subject are extracted by the webcam camera sensors and pre-processed, they are compared with the sample images. This study adopted the simple calculation method of mean square error (MSE), as expressed in Equation (1) for the contrast calculation between the detected hair images and sample images. In Equation (1), W and H are denoted as the width and height of image respectively, $Image_{ij}$ is the pixel (i, j) of input image, and P_{ij}^k is the pixel (i, j) of the k th sample image. Therefore, a 4×7 matrix can be acquired, as shown in Figure 5.

$$MSE_k = \frac{1}{W * H} \sum_{i=1}^W \sum_{j=1}^H (Image_{ij} - P_{ij}^k)^2 \tag{1}$$

Based on this matrix, the minimum value is selected as the output result, but it is dissatisfactory. The head type or shooting position of the subject may cause a small gap,

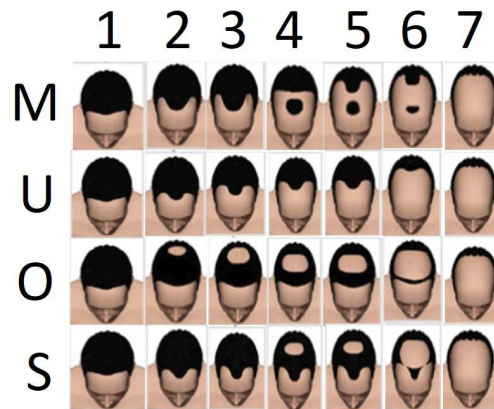


FIGURE 3. Norwood-Hamilton scale model

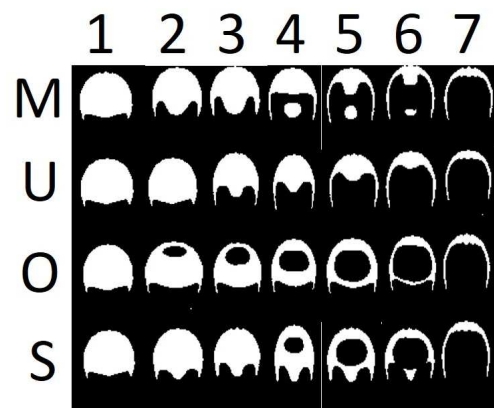


FIGURE 4. Pattern binarization images of the Norwood-Hamilton scale model







	1	2	3	4	5	6	7
M	3.1057	3.1044	3.2767	3.1155	3.0108	2.9176	2.6433
U	3.1211	2.9673	3.0629	3.0713	3.0434	2.6658	2.5990
O	3.17	2.6638	2.5195	2.3167 	2.1557 	2.4963 	2.6043
S	3.1641	2.9436	3.0778	2.6547	2.3105 	2.4720 	2.8642

FIGURE 5. The table of hair detection result

affecting the judgment results. Therefore, the first three minimum values are output in this study as the possible judgment results, and then a vote is cast against the baldness phase and baldness type according to the value position. For instance, if three values are located in (O type, Phase 4), (O type, Phase 5) and (syndrome type, Phase 5), respectively, it is judged that the baldness status belongs to O type and Phase 5, as described in Figure 5. In the column 6 and type of O and S of Figure 5, the output results of the fourth and fifth values are presented. It can be seen from Figure 5 that an output of more than three rank values will lead to an erroneous judgment. Therefore, a satisfactory result can be obtained when only the first three values are output. Additional experimental data are presented in Section 4.

3.3. Detection of scalp status. A color histogram is used to analyze a color image and recognize the shape and texture of objects because they are rotary, invariant to scaling, and immune to noise. In addition, in consideration of the implementation of the design, a real-time detection system can be realized because of the simplicity of the algorithm. Therefore, the histogram back projection method described in [22] was used to detect scalp in the RGB color space. The feature emphasized by this method and the object to be detected are highly correlated. Each pixel correlation is calculated through the histogram back projection technique, with the feature being determined according to the importance of the target object. Subsequently, the probability is output to determine the shape or texture to which the pixel belongs. The collected patterns of detection form the characteristic pixel region in the experimental database of the scalp status detection.

First, the histograms of input image I and pattern image P are calculated in the RGB color space, and then histogram ratio R between pattern sample P and input image I is computed. The purpose of this is to create a look-up table to replace an image and where its image pixel value signifies the level of correlation in the searching pattern sample. Then, the histogram is projected back to the image. Each pixel (x, y) of the color i in the original image is replaced by its histogram ratio. A higher value of the ratio identifies its expected location, and the corresponding mathematical expression is given in Equation (2).

$$R_i = \min \left[\frac{I_i}{P_i}, 1 \right] \quad (2)$$

where i signifies the index of one bin. Then this histogram ratio R is projected back to the image, i.e., the image pixel value is replaced by R 's value according to the index, and

the expression is shown in Equation (3).

$$b_{xy} = R_{h(I_{x,y})} \quad (3)$$

where $I_{x,y}$ is the color value of (x, y) of the input value and $h(I_{x,y})$ is the bin corresponding to $I_{x,y}$. Lastly, threshold processing is performed against b_{xy} of projected image and the peak value of the most possible position of the pattern sample object is recognized.

3.4. Parameter adjustment based on different lighting conditions. The color used for the histogram back projection technique is chosen based on the chromaticity, such that detecting the texture of the objects is very simple and fast. It has some congenital advantages in a real-time detection system. The limitation in this technique is also obvious. First, the effects depend on the pattern samples used. In this aspect, a large amount of data of different pattern samples are used to improve the overall detection accuracy. The algorithm used here also depends on the threshold technology to export the binary image. Therefore, different threshold technologies will generate different outcomes.

The images in the collected data were extracted under different lighting conditions and environments. A standard color inspector is used as the reference for color correction in professional devices. However, there is no standard color inspector for our collected data and system. Therefore, in the absence of a color inspector, in this research, we proposed the concept of using image color differences to evaluate the lighting condition. The method of supervised learning SVM [23] was adopted to train light conditions to be the lighting category to further adjust the parameters according to the category of the input image.

First, a scalp image is extracted in the experiment via a Universal Serial Bus (USB) microscope, and referential image basis I_b is generated for the scalp image, to be used as the basis of the color inspector. Let $I_{b(x,y)}$ and $I_{L_i(x,y)}$ be the image pixel shot under the lighting environment of b and L_i , respectively, corresponding to the chromaticity of the color coordinates in the CIE xyY color space. $D_{L_i(x,y)}$ is the pixel value difference between $I_{L_i(x,y)}$ and $I_{b(x,y)}$. The average of the entire difference value image is taken as the eigenvalue f_{L_i} , and the expression is given in Equation (4). When the lighting conditions become similar, its value reaches $f_{L_i} \cong f_{L_j}$. If the lighting conditions are different, f_{L_i} will also be different.

$$f_{L_i} = \frac{1}{W * H} \sum_{x=1}^W \sum_{y=1}^H D_{L_i(x,y)} = \frac{1}{W * H} \sum_{x=1}^W \sum_{y=1}^H (I_{L_i(x,y)} - I_{b(x,y)}) \quad (4)$$

To demonstrate the hypothesis, the collected scalp data are divided into three types of different lighting information, as illustrated in Figure 6. f_{L_i} of each image is calculated according to Equation (4) and all f_{L_i} are drawn in the color coordinates. Figure 6 proves our idea. Based on the different values of images, different lighting conditions can be classified. It is observed from Figure 6 that even if the average pixel of the scalp difference value varies from person to person, the color has a similar f_{L_i} under the same lighting condition. Then, an SVM classifier trained by f_{L_i} eigenvalues is used to predict the current lighting condition and this information is used to adjust parameter threshold. In our work, it is a simple way to extract the features of lighting condition for training an SVM classifier. Add to this, according to the types of lighting condition, we easily adjust the parameters in the detection process. When the user uses the microscope to scan the scalp seen in Figure 7, our system will automatically capture the image and calculate the lighting eigenvalue. Through the trained SVM classifiers seen in Figure 6, our system will estimate the lighting condition. Each lighting condition corresponds to a set of parameters for back project calculation and Otsu thresholding method. Given an approximated lighting

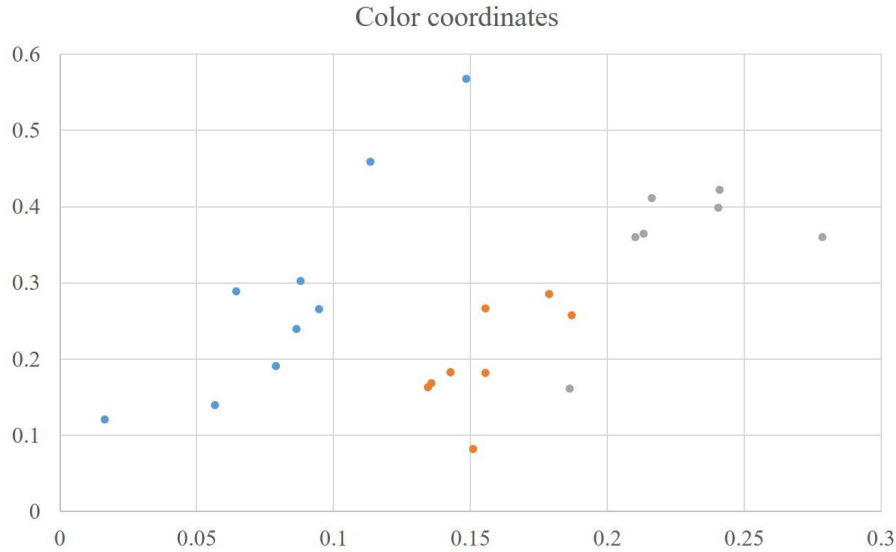


FIGURE 6. Color coordinates of scalp images captured under different light conditions



FIGURE 7. Proposed system

condition, we then choose the approximated parameters to evaluate the status of scalp. According to the experimental results, threshold adjustment with the use of this method has a significant effect.

4. Experimental Result. To evaluate the efficiency of our proposed detection method, we used the NVidia Jetson TK1 platform similar to [26]. The webcam and UPMOST (UPG622) microscope camera sensor were used to construct a hair and scalp analysis system, as shown in Figure 7. In addition to the camera sensors, a keyboard and mouse were provided to operate the user interface. Hundred baldness and scalp pictures were collected on the network to establish the experimental database respectively, as shown in Figure 8 and Figure 9. According to the data collected, the lighting conditions were classified into three types: slightly yellow, slightly white, and slightly red. With the addition of the lighting condition extracted by our own system, there were totally four types. The scalp status was classified into oily scalp, allergic/red, swollen scalp, and dry/keratinization scalp.

4.1. Experimental result of detecting baldness status. Generally, it is easy to judge the detection of M type baldness, as shown in Figure 10. In the first two output results, a highly accurate prediction result is obtained. According to Figure 11, thin hair is judged

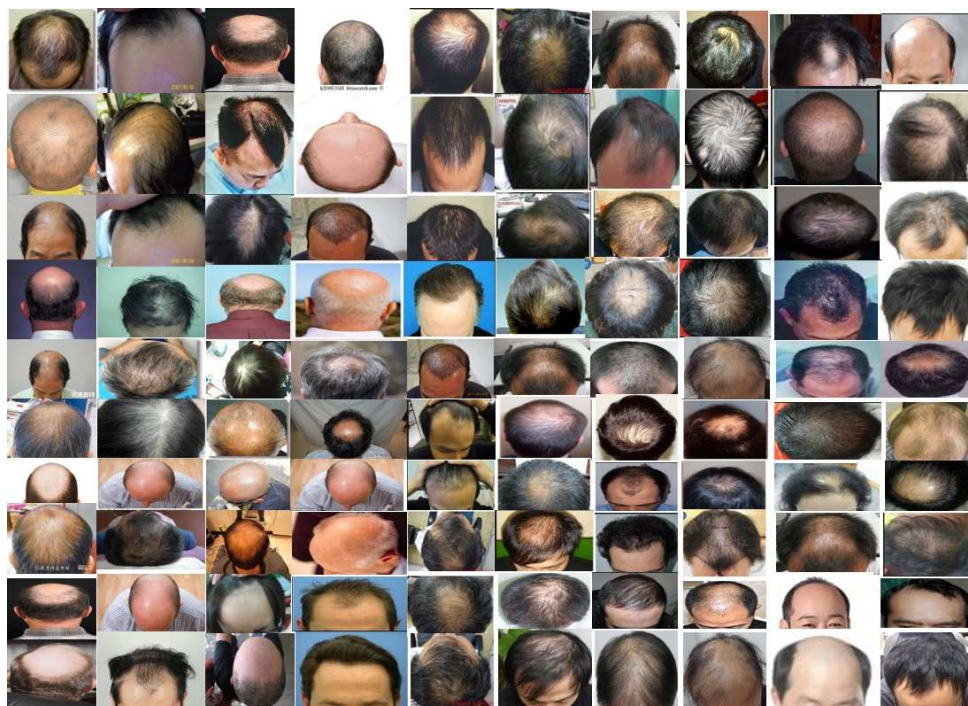


FIGURE 8. The collected data of baldness



FIGURE 9. The collected data of scalp

to be Phase 7 of baldness, but the type is difficult to guess because the hair is too sparse. The type in Figure 12 must be judged correctly in this study because this type belongs to one of baldness types; however, it is difficult to detect it correctly.

For this reason, the first three most possible results were output by our system design to improve the overall judgment efficiency. Figure 13 shows that this baldness type does not belong to any of the baldness models. Therefore, the judgment effect is sometimes dissatisfactory.

The experimental results targeting the collected baldness database are shown in Table 1. According to the experimental data, if only one or two of the most possible results are obtained, the recognition rate is not high, only 51% and 78%. If four or five most possible results are chosen, the recognition rate is 94% to 95%, but the output results (the 4th and 5th possible patterns) are usually wrong. Such phenomenon can be seen from Figures 10 to 13. Therefore, it is best to output the first three most possible results.

	1	2	3	4	5	6	7
M	1.8529	1.2919	1.0896	1.4864	2.1449	2.2614	2.3649
U	1.7273	1.6970	1.3534	1.5081	1.8497	2.1295	2.4016
O	1.7737	1.3798	1.8303	1.951	2.1099	2.1099	2.3995
S	1.8	1.5412	1.5398	2.9014	2.3100	2.311	2.3386

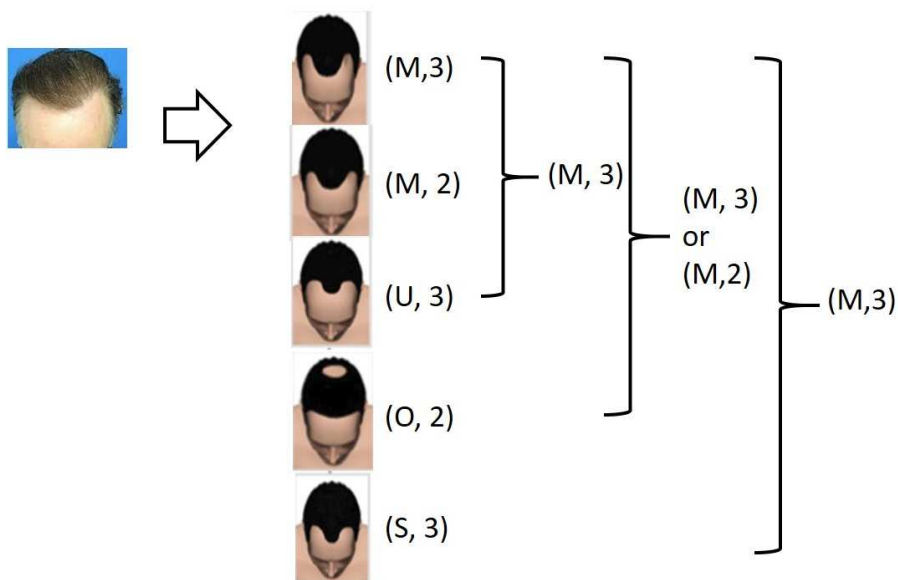


FIGURE 10. M type of bald hair

	1	2	3	4	5	6	7
M	2.4651	2.2947	2.3297	1.9105	1.5463	1.0766	0.775
U	2.4651	2.6363	2.1634	1.9725	1.3668	1.2574	0.8507
O	2.4485	2.3397	2.1104	1.9067	1.6059	1.1583	0.9343
S	2.4194	2.4489	2.4208	2.3128	1.8587	1.326	0.8896

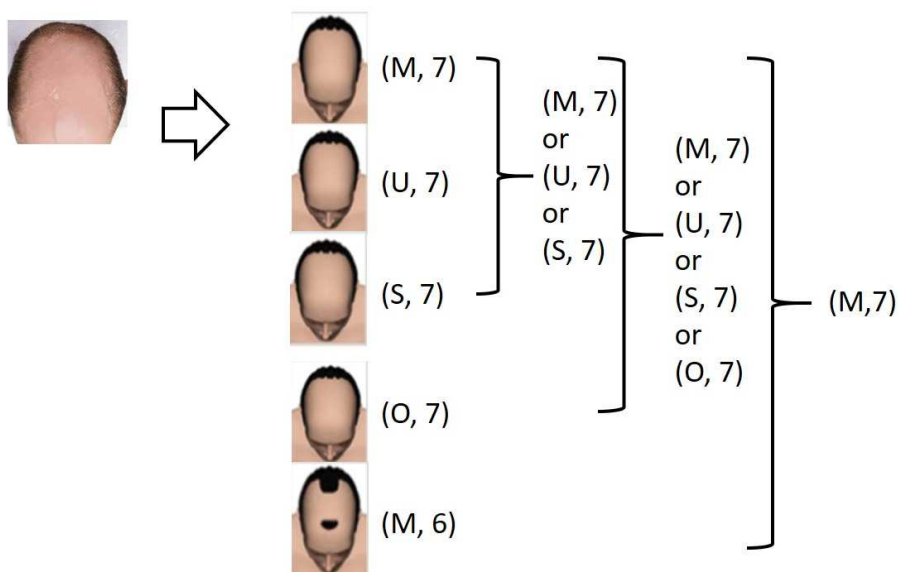


FIGURE 11. Rare hair

	1	2	3	4	5	6	7
M	3.1057	3.1044	3.2767	3.1155	3.0108	2.9176	2.6433
U	3.1211	2.9673	3.0629	3.0713	3.0434	2.6658	2.5990
O	3.17	2.6638	2.5195	2.3167	2.1557	2.4963	2.6043
S	3.1641	2.9436	3.0778	2.6547	2.3105	2.4720	2.8642

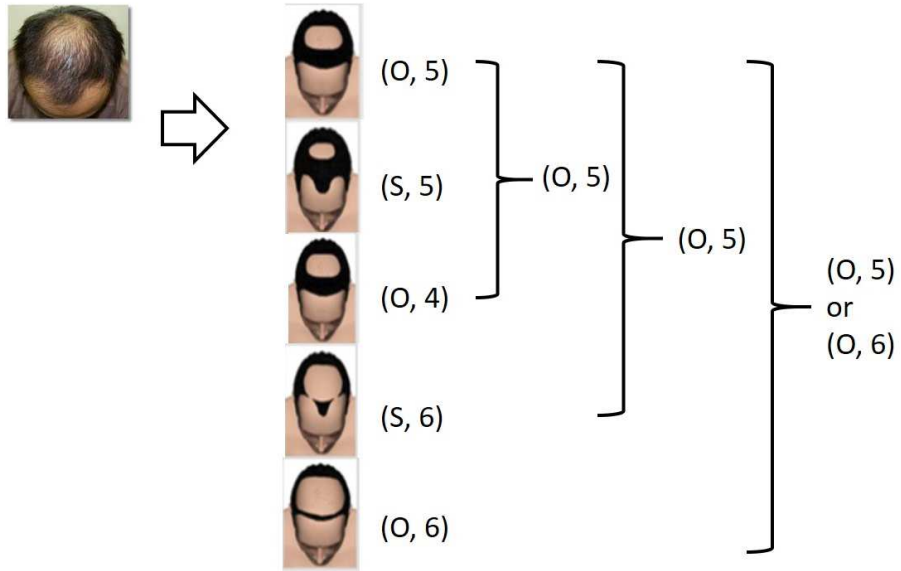


FIGURE 12. Syndrome type of bald hair

	1	2	3	4	5	6	7
M	3.1584	3.3225	3.4541	3.2694	3.0202	2.9039	2.6382
U	3.1994	3.0328	3.2486	3.1358	3.0012	2.7580	2.6229
O	3.3065	2.8836	2.6891	2.6346	2.4578	2.5778	2.6202
S	3.205	3.1428	3.186	2.9285	2.5626	2.5682	2.6206

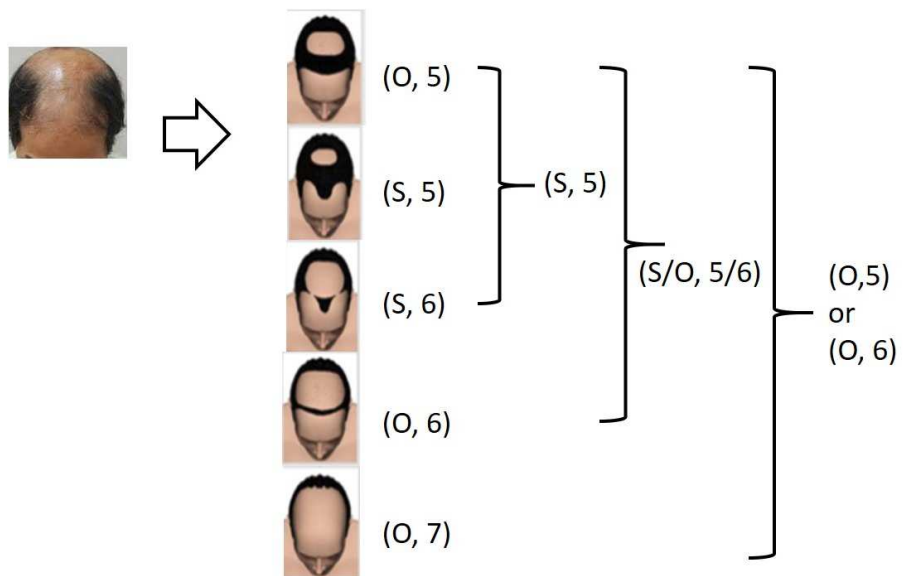


FIGURE 13. Hair type is out of the model.

TABLE 1. Accuracy of detection of bald hair type

Number of most possible results	1	2	3	4	5
Accuracy (%)	51	78	91	94	95

4.2. Experimental result of detecting scalp status. According to the data of scalp collected, the lighting conditions were classified empirically by ourselves into three types: slightly yellow, slightly white, and slightly red. With the addition of the lighting condition extracted by our own system, there were totally four classes. Each class in a row is represented respectively seen in Figure 9. The lighting condition in our own system is also to be used as referential image basis of the color inspector. All the experimental data are converted to CIE xyY color space and then according to Equation (4), they are calculated to lighting eigenvalues. By using the lighting eigenvalues, we trained the SVM classifier as illustrated in Figure 6. It is observed from Figure 6 that different lighting conditions can be classified. Then we manually set up a set of parameters corresponding to each class for back project calculation and Otsu threading method. When a test image is inputted, we can easily set the parameters of algorithm by the lighting condition information.

The histogram back projection technique was used to detect the scalp status. This experiment considered oily, allergic/red, swollen, and dry/keratinization scalps as the pattern samples, and the experiment was conducted according to the parameters adjusted by the lighting conditions. If the parameters are adjusted or selected in the absence of lighting conditions, the results will be quite different with the same parameters. Figure 14 and Figure 15 respectively describe that there is a significant difference in the status presented by the red and swollen scalps in the size of the bins from 2 to 8 scalps. In Figure 14, a better result is obtained when the parameter is 2; in Figure 15, a better result is acquired when the parameter is 7 or 8. Table 2 shows the overall experimental results, illustrating that a significant enhancing effect can be achieved when the parameter is adjusted according to the lighting conditions. The improvements are about 184%, 78% and 81% respectively. However, the accuracy rates under three conditions are not high enough. In the oily scalp status, it is vulnerable to the light reflection. Without the adjustment of parameter, we could see the accuracy rate is very low. Therefore, by applying to the adjustment of parameters, the accuracy rate is increasing effectively. The lighting condition is the most important in the scalp diagnosis system. The pictures of experiment collected on the network are various. We empirically classified them to three types of lighting condition. From the result of Table 2, the most possible reason causing the accuracy rates are not high enough would be the classification of lighting conditions. The second reason would be the hair obstacle. The preprocessing of hair segmentation is useful for clinical diagnosis of scalp. However, our target goal is to design a simple

TABLE 2. Performance with/without parameter adjustment for lighting condition

Situation	Parameter setup	Precision	Recall	Accuracy
oily scalp	default	42.37%	37.88%	25%
	with adjustment	74.74%	93.42%	71%
allergic/red and swollen	default	62.66%	65.28%	47%
	with adjustment	93.44%	89.36%	84%
dry and cuticularized	default	69.35%	53.09%	43%
	with adjustment	83.87%	91.76%	78%

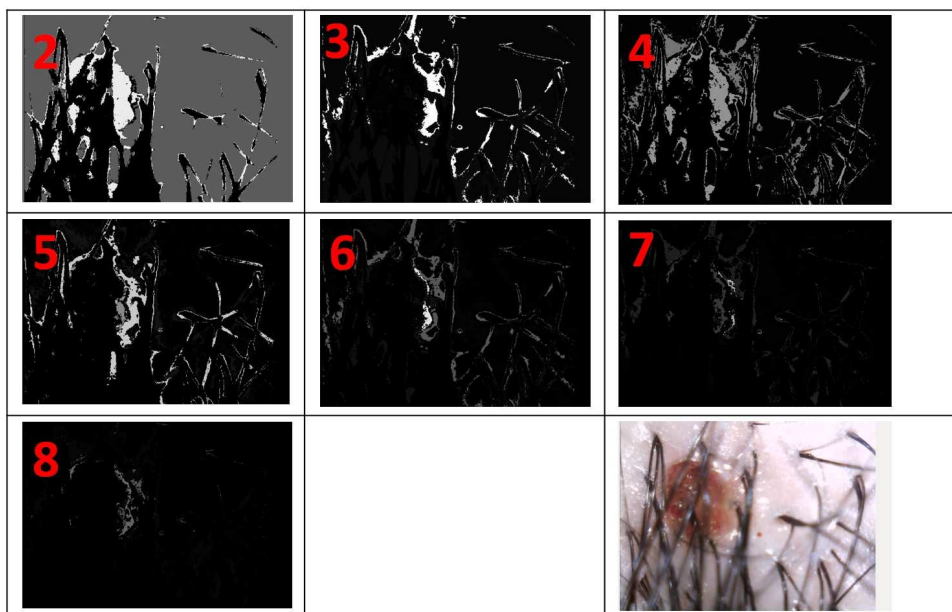


FIGURE 14. Image of scalp status 1

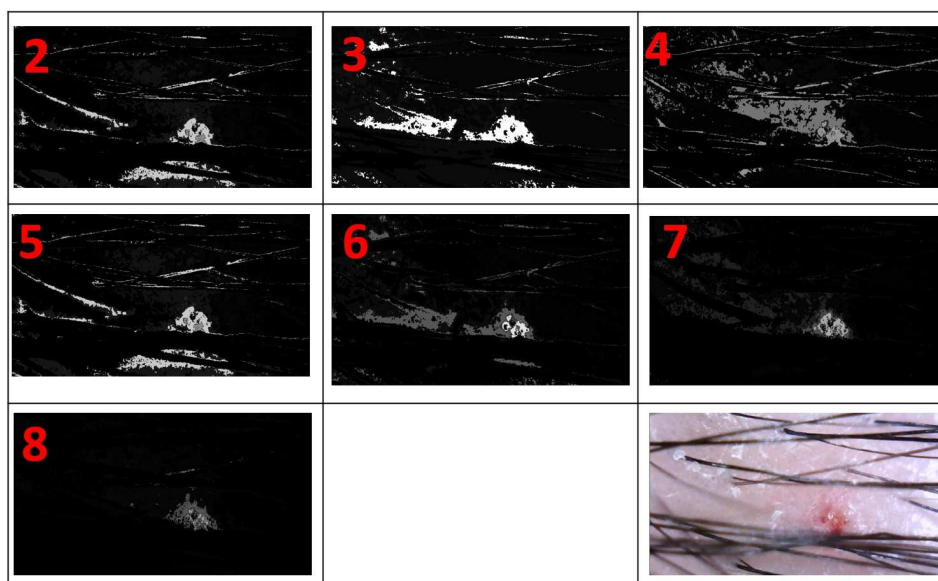


FIGURE 15. Image of scalp status 2

and fast diagnosis system. Therefore, we do not use the hair segmentation and removal process on our system. In the future work, we would design the consistent environment for collecting the experimental pictures and improve the accuracy rate. Add to this, we would consider the preprocessing of hair segmentation and removal for analyzing scalp to increase the robustness of the system.

5. **Conclusions.** In this study, a simple hair and scalp self-diagnosis embedded system was implemented in which webcam and microscope sensors were used to extract images. In regard to the diagnosis of hair status, the baldness status was determined for hair of users according to the Norwood-Hamilton scale model that was also used as a reference for users to utilize the golden phase for treatment. Simultaneously, the effects of images

taken under different lighting conditions were analyzed to adjust the parameters and detect scalp status effectively. The accuracy rate and precision/recall were calculated to measure the efficiency. The experimental results demonstrated this system as a valuable solution for human hair and scalp diagnosis.

Acknowledgment. This research is financially supported by the Ministry of Science and Technology of Taiwan (under grants No. 1042221-E-006-119-MY3 and No. 104-3115-E-194-001).

REFERENCES

- [1] H. Chen and S.-C. Zhu, A generative sketch model for human hair analysis and synthesis, *IEEE Trans. Pattern Anal. Mach. Intell.*, vol.28, no.7, pp.1025-1040, 2006.
- [2] M. Guarrera, P. Cardo, P. Arrigo and A. Rebori, Reliability of Hamilton-Norwood classification, *International Journal of Trichology*, vol.1, no.2, pp.120-122, 2009.
- [3] M. Gupta and V. Mysore, Classifications of patterned hair loss: A review, *Journal of Cutaneous and Aesthetic Surgery*, vol.9, no.1, pp.3-12, 2016.
- [4] H.-C. Shih, An unsupervised hair segmentation and counting system in microscopy images, *IEEE Sensors Journal*, vol.15, no.6, pp.3565-3572, 2015.
- [5] H.-C. Shih and B.-S. Lin, Hair segmentation and counting algorithms in microscopy image, *Proc. of IEEE ICCE*, Las Vegas, NV, USA, 2014.
- [6] H. Kim, W. Kim, J. Rew, S. Rho, J. Park and E. Hwang, Evaluation of hair and scalp condition based on microscopy image analysis, *International Conference on Platform Technology and Service (PlatCon)*, 2017.
- [7] P. Schmid-Saugeon, J. Guillod and J.-P. Thiran, Towards a computer-aided diagnosis system for pigmented skin lesions, *Comput. Med. Imag. Graph.*, vol.27, no.1, pp.65-78, 2003.
- [8] C.-K. Yeh, P. K. Jayaraman, X. Liu, C.-W. Fu and T.-Y. Lee, 2.5D cartoon hair modeling and manipulation, *IEEE Trans. Visualization and Computer Graphics*, vol.21, no.3, pp.304-314, 2015.
- [9] J. Yu and L. Li, A vivid visual emotion synthesis system: From face to hair, *IEEE the 13th International Conference on Signal Processing (ICSP)*, 2016.
- [10] L. Wang, Y. Yu, K. Zhou and B. Guo, Example-based hair geometry synthesis, *Proc. of ACM SIGGRAPH*, 2009.
- [11] I. Ahn and C. Kim, Face and hair region labeling using semi-supervised spectral clustering-based multiple segmentations, *IEEE Trans. Multimedia*, vol.18, no.7, pp.1414-1421, 2016.
- [12] M. Svanera, U. R. Muhammad, R. Leonardi and S. Benini, Figaro, hair detection and segmentation in the wild, *IEEE International Conference on Image Processing (ICIP)*, 2016.
- [13] H. Proença and J. C. Neves, Soft biometrics globally coherent solutions for hair segmentation and style recognition based on hierarchical MRFs, *IEEE Trans. Information Forensics and Security*, vol.12, no.7, pp.1637-1645, 2017.
- [14] P. Julian, C. Dehais, F. Lauze, V. Charvillat, A. Bartoli and A. Choukroun, Automatic hair detection in the wild, *Proc. of the 20th IEEE ICPR*, pp.4617-4620, 2010.
- [15] D. Wang, S. Shan, H. Zhang, W. Zeng and X. Chen, Isomorphic manifold inference for hair segmentation, *Proc. of the 10th IEEE Automat. Face Gesture Recognit. (FG)*, pp.1-6, 2013.
- [16] S. Joseph and J. R. Panicker, Skin lesion analysis system for melanoma detection with an effective hair segmentation method, *International Conference on Information Science (ICIS)*, 2017.
- [17] N. H. Nguyen, T. K. Lee and M. S. Atkins, Segmentation of light and dark hair in dermoscopic images: A hybrid approach using a universal kernel, *Proc. of SPIE, Med. Imag.*, vol.7623, 2010.
- [18] A. Huang, S.-Y. Kwan, W.-Y. Chang, M.-Y. Liu, M.-H. Chi and G.-S. Chen, A robust hair segmentation and removal approach for clinical images of skin lesions, *Proc. of the 35th Annu. Int. Conf. IEEE EMBS*, pp.3315-3318, 2013.
- [19] R. Lionnie and M. Alaydrus, An analysis of Haar wavelet transformation for androgenic hair pattern recognition, *International Conference on Informatics and Computing (ICIC)*, 2017.
- [20] R. Hoffmann, TrichoScan. A new instrument for digital hair analysis, *Hautarzt*, vol.53, no.12, pp.798-804, 2002.
- [21] R. O. Duda and R. E. Hart, Use of the Hough transformation to detect lines and curves in pictures, *Commun. ACM*, vol.15, no.1, pp.11-15, 1972.

- [22] M. J. Swain and D. H. Ballard, Color indexing, *International Journal of Computer Vision*, vol.7, no.1, pp.11-32, 1991.
- [23] C. C. Chang and C. J. Lin, *LIBSVM – A Library for Support Vector Machines*, <http://www.csie.ntu.edu.tw/~cjlin/libsvm/>.
- [24] N. Otsu, A threshold selection method from gray-level histograms, *IEEE Trans. Syst., Man, Cybern.*, vol.9, no.1, pp.62-66, 1979.
- [25] Arthur and S. Vassilvitskii, K-means++: The advantages of careful seeding, *Proc. of the 18th Annual ACM-SIAM Symposium on Discrete Algorithms*, 2007.
- [26] <http://www.nvidia.com/object/jetson-tx1-dev-kit.html>.